International Journal of Information Technologies and Systems Approach
Volume 16 • Issue 2

Optimization of Cogging Torque Based on the Improved Bat Algorithm

Wenbo Bai, College of Electricity & New Energy, China Three Gorges University, China*
Huajun Ran, College of Electricity & New Energy, China Three Gorges University, China

ABSTRACT

Permanent magnet motors have the advantages of high output torque, high efficiency, and low noise, but the cogging effect is obvious. The 24-slot 4-pole surface-mounted permanent magnet synchronous motor is taken as an example to reduce the cogging torque of permanent magnet synchronous motors. Firstly, the generation mechanism of cogging torque is analysed based on the energy method, and the pole arc coefficient, air gap length, magnetic pole eccentricity, permanent magnet thickness, and slot opening width are determined as optimisation parameters. Then, a cogging torque optimisation method is further proposed based on the Taguchi method and the response surface method, and the bat algorithm with the Lévy flight feature is applied to obtain the optimal solution for the response surface model. Finally, finite element software is used to simulate the optimal motor model. The experimental results show that the efficiency of the motor solved by optimal parameters is increased by 1.6%, the cogging torque is reduced by 82.16%, and the torque ripple is reduced by 8.2%. The optimisation of cogging torque in this paper avoids fluctuations in torque, reduces motor vibration and noise, and improves the control characteristics of the permanent magnet motors drive system, operational reliability, and low-speed performance in the motor speed control system and high accuracy positioning in the position control system.

KEYWORDS:

Cogging Torque, Taguchi Method, Response Surface, Bat Algorithm, Lévy Flight

INTRODUCTION

With the deterioration of the natural environment and the scarcity of fossil energy, it is increasingly important to protect the environment, save energy and reduce emissions to achieve sustainable development. The use of motors is increasing in the field of new energy, especially permanent magnet synchronous motors (PMSM), which are widely used due to their slip-ring and brushless structure, low noise level, high output torque and high efficiency (Qiu, 2020). However, due to the presence of cogging torque, permanent magnet motors can have large torque fluctuations during operation, bringing noise and vibration, affecting the motor's operating performance and control accuracy,

DOI: 10.4018/IJITSA.323442 *Corresponding Author

reducing the life of the motor and increasing costs (Hu et al., 2020). It is particularly important to reduce the cogging torque of PM motors because it is unavoidable.

At present, there has been a great deal of research to find ways to achieve the weakening of slot torque by optimising the structural parameters of different parts of the motor, such as arc coefficient (Wang et al., 2005; Yang et al., 2007), skewed pole (Jeihoon et al., 2016), magnetic pole eccentricity (Song et al., 2004) and stator teeth notching auxiliary slot (Wang et al., 2002). These methods optimised a single structural parameter, which can suppress the cogging torque. However, they also had problems, such as reduced torque density and increased cogging losses. In order to solve the problems caused by the optimisation of a single structural parameter, some scholars have optimised multiple parameters simultaneously, which not only reduces the cogging torque but also improves the performance of the motor to a certain extent. Yao (2023) used a structural combination of different slot widths and unequal-thickness permanent magnets to effectively reduce the cogging torque, but no method was given to determine the optimal combination of slot width and unequal-thickness permanent magnets. Yang et al. (2023) first optimised the symmetry coefficients of the rotor parameters Rib and HRib and then improved the nonuniform air gap, which can effectively reduce the cogging torque of the built-in V-shaped PM motor. In the literature (Ma et al., 2023), the permanent magnets were first segmented, and then the segmented permanent magnets were designed into a diagonal pole structure. Although the weakening of the cogging torque could be achieved, the method was complicated to produce. Feng et al. (2023) proposed a suitable combination of the pole arc coefficient and eccentricity of the permanent magnets to achieve the weakening of the slot torque. Ma et al. (2022) used a suitable combination of the pole arc coefficient of the permanent magnets and different tooth shapes and tooth widths of the stator to optimise the slot torque, and Jia et al. (2013); Deng et al. (2022); Guo et al. (2022) and Wang et al. (2016) proposed the Taguchi method to optimise multiple parameters of the permanent magnet motor to achieve the weakening of the slot torque. Yang et al. (2022) reduced the cogging torque of the built-in V-type permanent magnet motor by combining the uneven air gap structure and magnetic isolation bridge. Zhang et al. (2020) studied the influence of permanent magnet remanence, number of chutes and slot width on cogging torque for permanent magnet motors. Wang et al. (2021) proposed an optimisation method based on embedded magnetic pole offset and uneven air gap eccentric rotor to weaken the cogging torque of double-layer embedded PMSM.

Although all of the above methods are able to reduce the cogging torque, they are unable to obtain the exact values of the optimisation parameters under the optimal objective. Yao (2022) used the Taguchi method to optimise the selected rotor parameters and then set the rotor eccentricity to weaken the cogging torque. Zheng et al. (2022) analysed the influence of single parameters, such as air gap, slot depth, pole-slot ratio and the number of auxiliary rotor slots on cogging torque. Li et al. (2022) studied the influence of shape, offset angle, width and depth of the rotor surface on the air gap density harmonics and cogging torque of motors. Although all these methods are able to reduce the cogging torque, they do not take into account the effect of the superposition of the parameters on the cogging torque due to the coupling of the motors. Zhou (2021) comprehensively considered and obtained the best pole arc coefficient, the appropriate notch width and the eccentricity of magnetic steel under the appropriate cogging torque through finite element simulation. However, the proposed combined optimisation algorithm still had the possibility of an optimal solution. In response to the problems of the abovementioned optimisation methods, it has been proposed to introduce optimisation algorithms into the field of tooth slot torque optimisation. Xv et al. (2020) analysed the effects of the permanent magnet arc coefficient, permanent magnet tilt pole, stator shoe width coefficient and stator shoe offset on the cogging torque of the YASA motor and established a response surface model using the above parameters that optimises the cogging torque using a genetic algorithm, which meets the desired objectives. Zou (2020) analysed the effect of slot width, permanent magnet gap and stator tooth eccentricity distance on cogging torque, and used an improved genetic algorithm combined with the finite element method to weaken the cogging torque. Li et al. (2021) used the response surface method and the maximum-minimum ant colony algorithm (ACA) to achieve multiobjective

optimisation of symmetrical V-shaped asynchronous start permanent magnet synchronisation. Zhou et al. (2020) and Luo & Chen (2021) used genetic algorithms (GAs) to optimise the cogging torque of permanent magnet motors.

The introduction of an optimisation algorithm not only allows the exact value of each parameter under the optimal objective to be obtained but also takes into account the coupling between the performance of each parameter of the motor. However, for the initial stage of the ant colony algorithm, the algorithm search time is long, the algorithm time complexity is high and the algorithm converges too quickly, causing the algorithm to be in a stop state. The genetic algorithm programming is complex, the algorithm search speed is slow and there is a certain dependence on the initial population selection and other problems. Compared with the aforementioned ACA and GA, the bat algorithm (BA) has been applied to PMSM parameter identification because of its simple structure, strong search capability, fewer adjustable parameters and strong robustness, but there are problems in the parameter search process, such as the ease to fall into local optimum, low search accuracy and early convergence. To address the problems of the BA, Lévy flight is introduced to improve the algorithm by replacing the individual bat's search for the optimal position according to the Lévy flight characteristics. This can help in generating a larger range of search, iteration and matching in the search process of the global optimal solution, thus preventing the individual bat from falling into the local optimal position to the greatest extent and improving the solution speed and convergence accuracy of the algorithm.

Based on the above studies, Taguchi's algorithm is better at finding the optimisation factors that have a significant influence on the optimisation objective but cannot find the optimal value of the optimisation parameters. The bat algorithm with Lévy flight characteristics can better find the optimal values of the optimisation parameters. This paper, taking the 24-slot, 4-pole surface-mounted permanent magnet synchronous motor as an example, first optimises the stator-rotor structure parameters of the permanent magnet synchronous motor by Taguchi's method. Then, the parameters that have a large influence on the optimisation target are taken for further optimisation, and the response surface method is used to fit the optimisation target into a mathematical model of the relevant optimisation parameters. Finally, the BA with a Lévy flight feature is used to optimise the above model and determine the parameter optimal value under the minimum cogging torque, thereby weakening the cogging torque of motors.

ANALYTICAL ANALYSIS OF COGGING TORQUE AND THE MAIN PARAMETERS OF MOTORS

The cogging torque is defined as the negative derivative of the magnetic field energy W with respect to the position angle α when the motor is not energised:

$$T_{cog} = -\frac{\partial W}{\partial \alpha}. \tag{1}$$

Regardless of saturation, assume that the magnetic permeability of the armature core is infinite. The magnetic field energy is approximately equal to the magnetic field energy in the air gap of motors and the permanent magnet, that is:

$$W \approx W_{airgap+PM} = \frac{1}{2\mu_0}\int_V B^2 dV, \tag{2}$$

where μ_0 is the air magnetic permeability. The distribution of the air gap magnetic density along the surface of the armature of a permanent magnet motor can be approximated as follows:

$$B\left(\theta,\alpha\right)=B_r(\theta)\frac{h_m(\theta)}{h_m(\theta)+\delta(\theta,\alpha)}, \tag{3}$$

where α is the angle between the centre line of a specified permanent magnet and the centre line of a specified tooth; $\theta=0$ is set on the pole centreline; B_r is the residual magnetism; h_m is the thickness of the permanent magnet and δ is the effective air gap length. Substitute (3) into (2) to obtain:

$$W=\frac{1}{2\mu_0}\int_V B_r^2(\theta)(\frac{h_m(\theta)}{h_m(\theta)+\delta(\theta,\alpha)})^2 dV\ . \tag{4}$$

Taking Fourier decomposition on $B_r^{\ 2}(\theta)$ and $(\frac{h_m(\theta)}{h_m(\theta)+\delta(\theta,\alpha)})^2$ yields:

$$B_r^2(\theta)=B_{r0}+\sum_{n=1}^{\infty}B_{rn}\cos 2np\theta \tag{5}$$

$$B_{r0}=\alpha_p B_r^2 \tag{6}$$

$$B_{rn}=\frac{2}{n\pi}B_r^2\sin n\alpha_p\pi \tag{7}$$

$$(\frac{h_m(\theta)}{h_m(\theta)+\delta(\theta+\alpha)})^2=G_0+\sum_{n=1}^{\infty}G_n\cos nq(\theta+\alpha) \tag{8}$$

$$G_0=(\frac{h_m}{h_m+\delta})^2 \tag{9}$$

$$G_n=\frac{2}{n\pi}(\frac{h_m}{h_m+\delta})^2\sin(n\pi-\frac{nq\theta_{s0}}{2}), \tag{10}$$

where α_p is the pole arc coefficient; p is the number of pole pairs; G_0 and G_n are the Fourier decomposition coefficients of air gap permeance square; G_n is the number of armature slots and θ_{s0} is the radian value corresponding to the width of stator slots.

Regardless of the chute, the expression for cogging torque is:

$$T_{cog(\alpha)}=\frac{nqL_{F_e}}{4\mu_0}(R_2^2-R_1^2)\sum_{n=1}^{\infty}nG_nB_{r\frac{nq}{2p}}\sin(nq\alpha) \tag{11}$$

$$B_{r\frac{nq}{2p}}=\frac{4p}{nq\pi}B_r^2\sin\frac{nq}{2p}\alpha_p\pi, \tag{12}$$

where L_{Fe} is the axial length of the armature core; R_1 is the outer diameter of rotors; R_2 is the inner diameter of stators and n is an integer such that $nq/2p$ is an integer.

Based on the above formulas, five parameters, pole arc coefficient α_p, air gap length δ, magnetic pole eccentricity h, permanent magnet thickness h_m and slot opening width b_s0, are selected as the final optimisation parameters. The initial parameters of motors are shown in Table 1. Figure 1 represents a distribution diagram of magnetic force lines for the PMSM. The magnetic force lines are evenly distributed, and the motor design is basically reasonable. The optimal shape for subdivision in Ansoft Maxwell 2D software is triangular, and the mesh subdivision of PMSM generated by automatic subdivision settings is shown in Figure 2.

Table 1. Main parameters of PMSM

Parameter	Parameter Value
Stator outer diameter/mm	120.00
Stator inner diameter/mm	75.00
Rotor outer diameter/mm	74.00
Rotor inner diameter/mm	24.00
Core axial length/mm	65.00
Rotate speed/(r·min-1)	1,500.00
Air gap length/mm	0.75
Permanent magnet thickness/mm	4.50
Pole arc coefficient	0.75
Slot opening width/mm	2.10
Magnetic pole eccentricity/mm	0.00

Figure 1. Distribution diagram of magnetic force lines

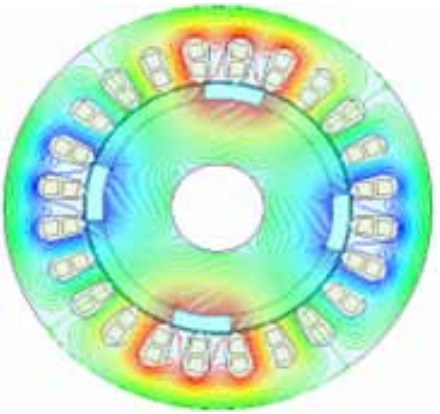

Figure 2. Mesh subdivision diagram

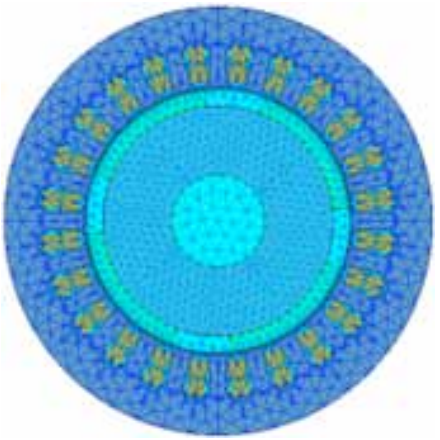

Motor Optimisation Process

Orthogonal Experimental Design and Results Based on the Taguchi Method

The Taguchi method is a local optimisation method proposed by Dr Genichi Taguchi to improve product quality and reduce the influence of various disturbances. The method is widely applicable and can simultaneously optimise multiple motor performance parameters. Orthogonal simulation experiments greatly reduce the number of trials and facilitate the rapid finding of optimal parameter combinations (Qiu, et al., 2020). The level values of optimisation parameters are shown in Table 2, according to the motor design manual (Tang, 1997).

According to the optimised parameters and the determined level values in Table 2, the experimental design principle of the Taguchi method and the principle of constructing orthogonal tables are used to build L25 orthogonal tables. Only 25 experiments are required to realize the multivariate optimised design, which significantly reduces the number of experiments and the degree of calculation (Chen et al., 2021). Moreover, 25 motor models corresponding to each group of experimental parameter levels are established in the finite element software, and the calculation and analysis of each motor model are performed. The experimental results are shown in Table 3.

Data Analysis of Experimental Results

The average value calculation and variance analysis are carried out according to the data results in Table 3 to obtain the impact and proportion of optimisation parameter changes on the optimisation objective.

First, the average value of analysis results for the optimised target finite element is obtained according to formula (13), and the calculated result is 95.84 mN·m.

$$m = \frac{1}{25}\sum_{i=1}^{25} S_i \,, \tag{13}$$

where m is the average value of the optimisation objectives and S_i is the target value for the i-th experimental optimisation. Then, the average value of optimisation parameters at different levels is calculated. For example, the air gap length δ is optimised at level 2 with the following equation for the mean target value:

$$T_{cog,avg,\delta,2} = \frac{1}{5}(S_2 + S_7 + S_{12} + S_{17} + S_{22}) \,. \tag{14}$$

The average value of optimisation objectives at different levels of each optimisation parameter can be calculated according to the above calculation methods, and calculation results are shown in Table

Table 2. Optimisation parameters and level values

Optimisation Parameter	Level 1	Level 2	Level 3	Level 4	Level 5
Pole arc coefficient	0.6	0.65	0.7	0.75	0.8
Air gap length/mm	0.5	0.75	1.0	1.25	1.5
Magnetic pole eccentricity/mm	11.0	11.75	12.5	13.25	14.0
Permanent magnet thickness/mm	4.5	4.75	5.0	5.25	5.5
Slot opening width/mm	2.1	2.20	2.3	2.40	2.5

Table 3. Orthogonal table and calculation results of the finite element

Experiment no.	Pole Arc Coefficient	Air Gap Length	Magnetic Pole Eccentricity	Permanent Magnet Thickness	Slot Opening Width	Cogging Torque/ (mN·m)
1	1	1	1	1	1	82.26
2	1	2	2	2	2	100.32
3	1	3	3	3	3	93.58
4	1	4	4	4	4	106.52
5	1	5	5	5	5	107.69
6	2	1	2	3	4	69.22
7	2	2	3	4	5	87.88
8	2	3	4	5	1	82.53
9	2	4	5	1	2	121.80
10	2	5	1	2	3	120.07
11	3	1	3	5	2	93.92
12	3	2	4	1	3	72.02
13	3	3	5	2	4	90.23
14	3	4	1	3	5	153.84
15	3	5	2	4	1	84.18
16	4	1	4	2	5	84.53
17	4	2	5	3	1	85.44
18	4	3	1	4	2	107.67
19	4	4	2	5	3	110.04
20	4	5	3	1	4	90.98
21	5	1	5	4	3	91.93
22	5	2	1	5	4	68.79
23	5	3	2	1	5	60.64
24	5	4	3	2	1	150.58
25	5	5	4	3	2	79.34

4. The pole arc coefficient has the smallest average value in cogging torque at level 5; air gap length, magnetic pole eccentricity and permanent magnet thickness have the smallest average value of cogging torque at level 2 and slot opening width has the smallest average value of cogging torque at level 4.

Variance (Var) can be calculated using formula (15) according to the average value of the above optimisation objective and the average value of each optimisation parameter at different levels. Moreover, the influence proportion of each optimisation parameter on optimisation objectives can be obtained. The calculation results are shown in Table 5.

$$Var = \frac{1}{5}\sum_{l=1}^{5}(T_{cog,avg,x,l} - m)^2 , \tag{15}$$

Table 4 The average value of each optimisation parameter at different levels of optimisation objectives

Optimisation Parameter	Level Value	Tcog, Avg/mN·m
Pole arc coefficient	1	98.07
	2	96.30
	3	98.84
	4	95.73
	5	90.26
Air gap length	1	84.37
	2	82.89
	3	86.93
	4	128.56
	5	96.45
Magnetic pole eccentricity	1	106.53
	2	84.88
	3	103.39
	4	84.99
	5	99.42
Permanent magnet thickness	1	109.15
	2	85.54
	3	96.28
	4	95.64
	5	92.59
Slot opening width	1	97.00
	2	100.61
	3	97.53
	4	85.15
	5	98.92

where x is the optimisation parameter and $T_{cog,avg,x,l}$ is the average value of optimisation objectives for the optimisation parameter x at the level l.

According to Table 5, changes in air gap length, magnetic pole eccentricity and permanent magnet thickness will cause large changes in cogging torque. Therefore, these three parameters are selected as further optimisation parameters.

Response Model Building

The response surface method was first proposed by Box and Wilson in 1951 as a statistical method for solving multivariate. There are two main types: central composite design and Box-Behnken design. Compared with the central composite design, the Box-Behnken design requires fewer trials. Therefore, this paper chooses the Box-Behnken design with level 3 (Hu et al., 2020). It can be seen from Table 4 that the mean values of cogging torque are the smallest at level 2 for air gap length, magnetic pole eccentricity and permanent magnet thickness. Thus, two symmetrical values are selected around

Table 5. The influence proportion of optimisation parameter changes on optimisation objectives

Optimisation Parameter	Var (10-4)	Proportion (%)
Pole arc coefficient	9.07	1.92
Air gap length	289.92	61.38
Magnetic pole eccentricity	84.39	17.87
Permanent magnet thickness	58.81	12.45
Slot opening width	30.14	6.38
Total	472.33	100.00

level 2 as the corresponding values of the next level number, and the redefined parameter levels are shown in Table 6.

The response model between the optimisation parameters and optimisation objectives can be expressed as follows:

$$y = c_0 + \sum_{i=1}^{3} c_i z_i + \sum_{i=1}^{3} c_{ii} z_i^{\,2} + \sum_{i=1}^{2} \sum_{j>i}^{3} z_i z_j + n\,, \tag{16}$$

where y is the response value; z is the independent variable; c is the coefficient to be determined and n is the error of fit.

Design-Expert.V8.0.6.1 software is used to automatically generate 17 experimental points after the model is established. The amplitude of cogging torque for each experimental point was calculated by the finite element method, as shown in Table 7, where A, B and C, respectively, represent air gap length, magnetic pole eccentricity and permanent magnet thickness.

The response surface model calculated from the experimental data in Table 7 is shown in Equation (17):

$$y = 4022.91 - 249.21A - 233.42B - 1060.98C + 1.17AB + 15.76AC + 0.15BC + 109.18A^2 + 9.88B^2 + 110.74C^2 \tag{17}$$

According to the response surface model, the relationship between the PMSM cogging torque and parameters A, B and C can be obtained, as shown in Figure 3. Figure 3 shows the response between the air gap length and magnetic pole eccentricity versus cogging torque. It can be seen from Figure 3 that as the air gap length increases, the cogging torque shows a tendency to decrease and then increase while being in the range of 0.6 to 0.9, where the cogging torque is at its minimum. Figure 4 shows the response between the air gap length and permanent magnet thickness versus cogging torque. In Figure 4, it is clear that the cogging torque decreases and then increases with an increase

Table 6. Optimisation parameter levels

Optimisation Parameter	Level –1	Level 0	Level 1
Air gap length	0.5	0.75	1.0
Magnetic pole eccentricity	11.0	11.75	12.5
Permanent magnet thickness	4.5	4.75	5.0

Table 7. The cogging torque of box-Behnken experimental points

Experiment no.	A/mm	B/mm	C/mm	Tcog/mN·m
1	1.00	11.75	4.50	65.97
2	0.75	12.50	5.00	67.41
3	1.00	12.50	4.75	66.09
4	0.75	11.75	4.75	53.47
5	1.00	11.00	4.75	66.05
6	0.75	11.75	4.75	53.47
7	0.75	11.75	4.75	53.47
8	0.75	12.50	4.50	65.73
9	0.50	11.00	4.75	66.03
10	0.50	12.50	4.75	65.19
11	0.75	11.00	4.50	64.52
12	0.50	11.75	5.00	66.47
13	0.75	11.75	4.75	53.47
14	0.50	11.75	4.50	65.19
15	1.00	11.75	5.00	71.19
16	0.75	11.75	4.75	53.47
17	0.75	11.00	5.00	66.17

in magnetic pole eccentricity and has a minimum value in the range of 11.3 to 12.2. Figure 5 shows the response between the magnetic pole eccentricity and permanent magnet thickness versus cogging torque. It shows that as the permanent magnet thickness increases, the cogging torque decreases and then increases, and there is a minimum value at a certain point in the range of 4.6 to 4.9. However, when the optimisation objective is minimised, an additional calculation is required to obtain the exact value of each optimisation parameter.

Figure 3. The response surface of A and B

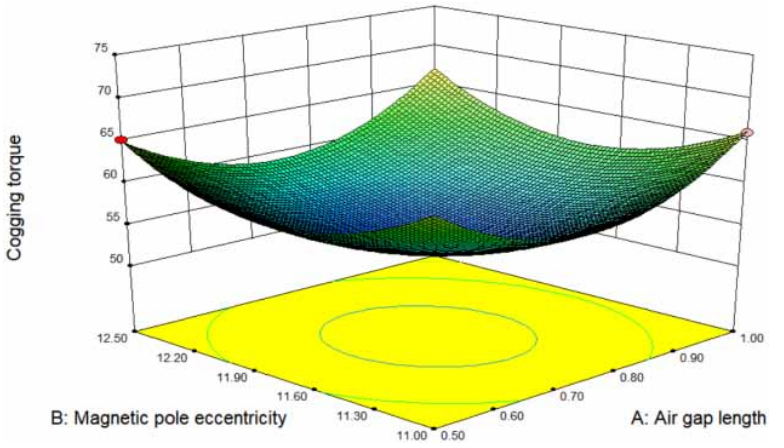

Figure 4. The response surface of A and C

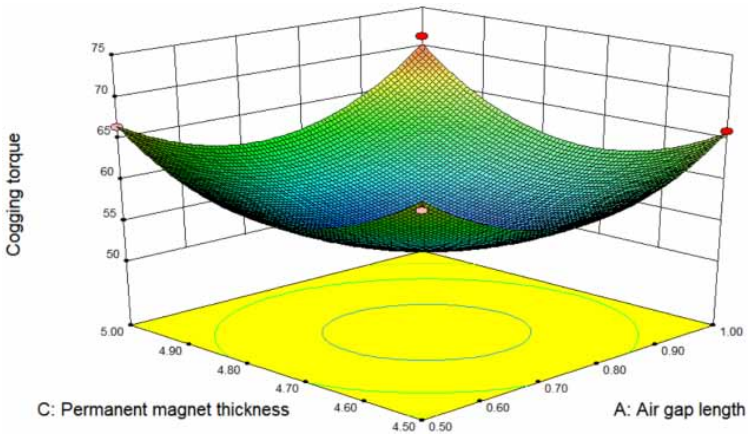

Figure 5. The response surface of B and C

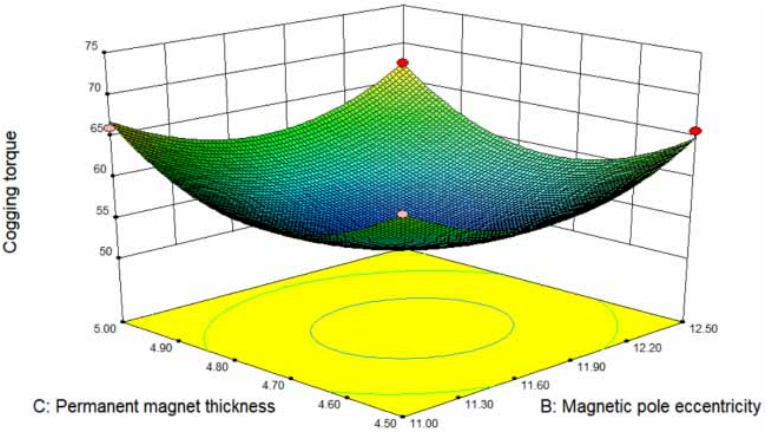

BA Optimisation With Lévy Flight Feature

Basic Intelligent Algorithms

Genetic Algorithm

GA is a type of randomised search method evolved from the law of evolution in the biological world (genetic mechanism of survival of the fittest). Its main features are to directly operate on structural objects; the absence of derivative and function continuity qualifications; the inherent and implicit parallelism and better global search capability; the use of probabilistic search methods, the ability to automatically obtain and guide the search space for optimisation and the adaptive adjustment of the search direction without the need to determine rules (Zhou et al., 2020). The flow chart of its algorithm is shown in Figure 6.

Ant Colony Algorithm

ACA is a bionic optimisation algorithm. Ants release pheromones along their path during foraging. Other individuals can exhibit intelligent foraging behaviour under the action of pheromones. In the ACA algorithm, the probability of transferring node i to node j can be calculated as follows:

Figure 6. Genetic algorithm flow chart

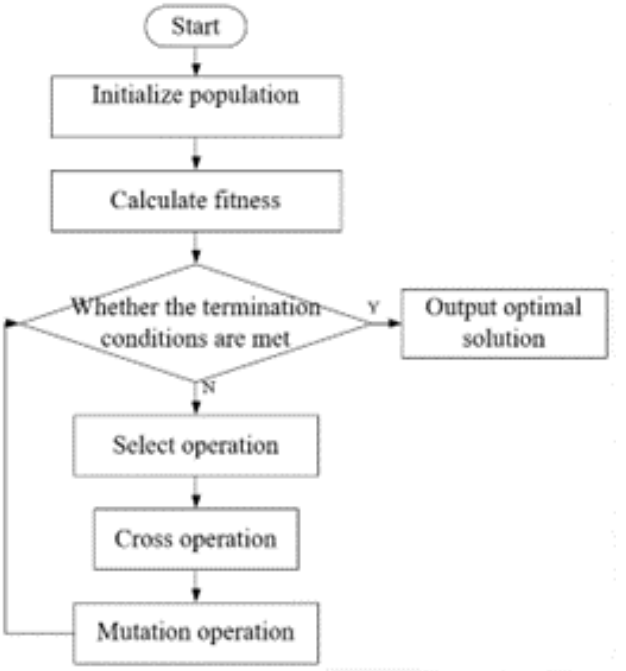

$$P_{ij}^{k}(t)=\begin{cases}\dfrac{\tau_{ij}^{\alpha}(t)\eta_{ij}^{\beta}(t)}{\sum_{s\in S}\tau_{is}^{\alpha}(t)\eta_{is}^{\beta}(t)}, j\in S\\ 0, \text{others}\end{cases}, \tag{18}$$

where $P_{ij}^{k}(t)$ represents the transition probability from ant k to the next node; α and β represent the weights of pheromone function and heuristic function, respectively; S represents the set of nodes that ant k can choose for the next step; $\tau_{ij}(t)$ represents the time t from point i to point j is the pheromone concentration on the path; $\eta_{ij}(t)$ represents the heuristic value on the path from point i to point j at the time t, $\eta_{ij}=1/d_{ij}$ and d_{ij} are the Euclidean distance between nodes i and j.

The pheromone update formula can be expressed as follows:

$$\tau(i,j)=(1-\rho)\cdot\tau(i.j)+\sum_{k=1}^{m}\Delta\tau_{k}(i,j) \tag{19}$$

$$\Delta\tau_{k}(i,j)=\begin{cases}(C_{k})^{-1}, (i,j)\in R^{k}\\ 0, \text{others}\end{cases}, \tag{20}$$

where ρ is the volatilisation coefficient of the pheromone and the range is from 0 to 1. The second half of Equation (19) is the amount of information added to the path after addressing.

Bat Algorithm

BA is a swarm intelligence algorithm that iteratively updates the pulse emission rate, loudness, speed and pulse frequency of each bat in the population when bats use echolocation to forage (Cui et al., 2021). The iterative formula of pulse frequency f_i, position x_i^t and velocity v_i^t of each bat is as follows:

$$f_i = f_{\min} + (f_{\max} - f_{\min})\beta \tag{21}$$
$$x_i^t = x_i^{t-1} + v_i^t \tag{22}$$
$$v_i^t = v_i^{t-1} + (x_i^{t-1} - x^*)f_i, \tag{23}$$

where f_i is the pulse frequency sent by the bat i; the minimum and maximum values of the frequency are f_{min} and f_{max}, respectively; $\beta \in [0,1]$ is a uniformly distributed random number; v_i^t and x_i^t denote the flight speed and position of the bat i at the moment t and x^* represents the current optimal position.

In the local search process of the algorithm, a random walk needs to be performed near the current optimal solution to generate a new solution (Xiong et al., 2017):

$$x_{new} = x^* + \varepsilon A^t, \tag{24}$$

where $\varepsilon \in [-1,1]$ is a uniformly distributed random number and A^t is the average loudness of bats in a generation t.

Moreover, iterative equations for pulse emissivity and loudness can be expressed as:

$$r_i^{t+1} = r_i^0(1 - e^{-\gamma t}) \tag{25}$$
$$A_i^{t+1} = dA_i^t, \tag{26}$$

where r_i^{t+1} and A_i^{t+1} represent the pulse emission rate and loudness of the $t+1$ generation; r_i^0 is the initial pulse firing rate and d and γ are adjustment coefficients.

Optimisation Comparison of Basic Intelligent Algorithms

The minimum value of the response surface model is solved using genetic algorithms ACA and BA according to the parameter range defined by the response surface and combined with Equation (17). The precise values of air gap length, magnetic pole eccentricity and permanent magnet thickness are determined. The results are shown in Table 8.

After genetic algorithm optimisation, the air gap length is 0.6 mm, the magnetic pole eccentricity is 11.9 mm, the permanent magnet thickness is 4.8 mm and the cogging torque is 55.15 mN·m. After ACA optimisation, the pole arc coefficient is 0.7 mm, the magnetic pole eccentricity is 11.9 mm, the permanent magnet thickness is 4.9 mm and the cogging torque is 45.98 mN·m. After BA optimisation, the air gap length is 0.7 mm, the magnetic pole eccentricity is 11.7 mm, the permanent magnet thickness is 4.7 mm and the cogging torque is 52.74 mN·m. It can be concluded that the optimisation performance of BA is better than the genetic algorithm and ACA.

Improved BA With Lévy Flight Feature and Optimisation Results

Compared with ACA and genetic group algorithm, BA has high applicability, strong optimisation performance, high accuracy and high computational efficiency. However, it cannot mutate during solution exploration. In addition, individual bats have a certain probability of falling into the optimal local position, causing the algorithm to easily fall into the local optimal. In addition, the pulse emission rate tends to the maximal (Zhang et al., 2021), and the loudness tends to zero at the later stage of iteration. If the excellent newly generated solution cannot be accepted because it does not meet the

Table 8. Optimisation results of cogging torque

Method	A/mm	B/mm	C/mm	Tcog/mN·m
Genetic algorithm	0.6	11.9	4.8	55.15
ACA	0.7	11.9	4.9	55.98
BA	0.7	11.7	4.7	52.74

conditions, the algorithm is premature. In this paper, Lévy flight behaviour is introduced to address the above problems, strengthen the algorithm to avoid local optimisation and strengthen the global search ability (Li et al., 2021).

The Lévy flight behaviour is part of a random wandering model. A random walk model is a mathematical form that describes a series of unstable moving trajectories. In the space of any dimension, a point is moved in any direction by a random step distance, and the step is repeated. From a mathematical point of view, the variation of the Lévy flight feature obeys Lévy distribution, which is a nonnormal random process (Zhang et al., 2021). In the process of searching for the optimal global solution, using the Lévy flight feature to replace the search for the best position for the bat individual can improve the optimisation range of the algorithm and prevent the bat individual from falling into the optimal local position. The speed and position of the improved BA are updated as follows:

$$x_i^{t+1} = x_i^t + Le'vy(\lambda) \otimes (x_i^t - x^*), \tag{27}$$

where *Lévy*(λ) is any search vector whose step size obeys *Lévy* distribution when the position is updated; λ is the scale parameter between [1, 3] and $\bigotimes$ represents the vector operation. The improved BA process is shown in Figure 7.

BA with the Lévy flight feature is used to solve the minimum value of the above response surface model. After optimisation, the air gap length is 0.7 mm, the magnetic pole eccentricity is 11.714 mm, the permanent magnet thickness is 4.732 mm and the cogging torque is 47.93 mN·m. Compared with the cogging torque of 268.67 mN·m before optimisation, the amplitude after BA optimisation is reduced by 80.37%. The amplitude of BA with the Lévy flight feature is reduced by 82.16% after optimisation, and the amplitude is reduced by 9.12% compared to the BA optimisation.

Simulation Analysis

A finite element model was built by Maxwell to verify the effectiveness of the proposed method, and the experimental results are shown in Table 9. After basic BA optimisation, the pole arc coefficient was 0.8, the air gap length was 0.7 mm, the magnetic pole eccentricity was 11.7 mm, the permanent magnet thickness was 4.7 mm, the slot opening width was 2.4 mm and the verification result of finite element analysis was 53.18 mN·m. The optimised pole arc coefficient with Lévy flight feature was 0.8, the air gap length was 0.682 mm, the magnetic pole eccentricity was 11.734 mm, the permanent magnet thickness was 4.783 mm, the slot opening width was 2.4 mm and the verification result of finite element analysis was 47.21 mN·m. The optimised cogging torque was similar to the verification result of the finite element analysis, indicating that the developed response surface model is accurate, and the optimal solution of motor parameters obtained using BA with the Lévy flight feature can weaken the cogging torque.

The cogging torque and torque ripple before and after motor optimisation at no load and up to 1,500 min-1 are shown in Figures 8 and 9, respectively. The optimised cogging torque was significantly reduced, mainly because changing the parameters of motors will change the magnetic permeability between the air gaps, effectively improving the air gap magnetic circuit (Li et al., 2021). Since the cogging torque is the main source of torque ripple, reducing cogging torque is effective in reducing

Figure 7. Flow chart of an improved BA

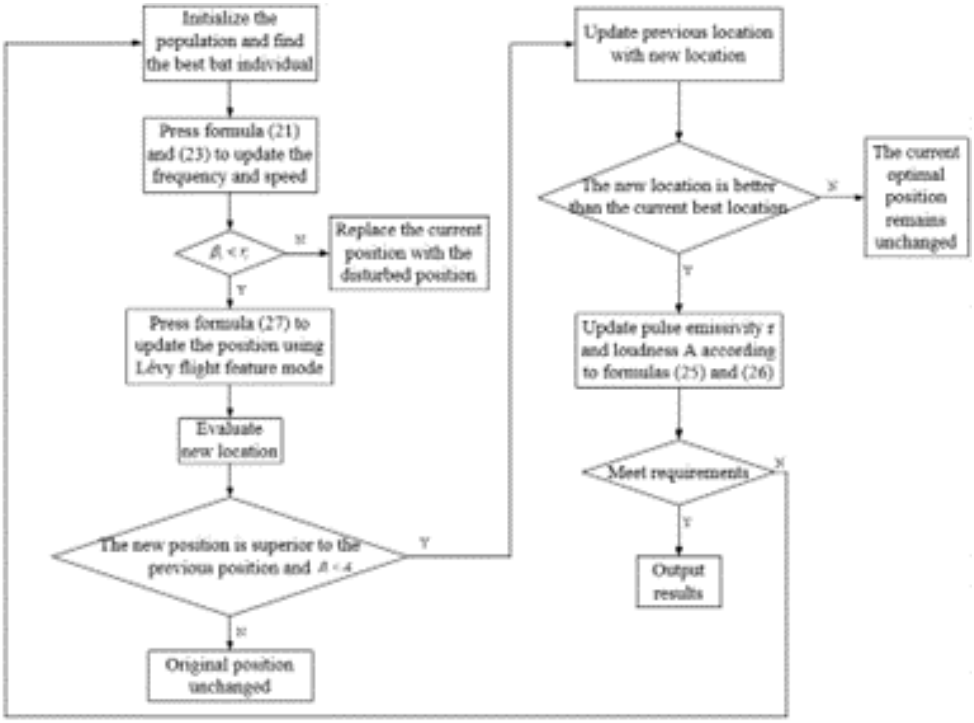

Table 9. Comparative verification results of finite element

Method	Pole Arc Coefficient	Air Gap Length	Magnetic Pole Eccentricity	Permanent Magnet Thickness	Slot Opening Width	Cogging Torque/mN·m
BA	0.8	0.7	11.700	4.700	2.4	52.74
Finite element	0.8	0.7	11.700	4.700	2.4	53.18
Improved BA	0.8	0.7	11.714	4.732	2.4	47.93
Finite element	0.8	0.7	11.714	4.732	2.4	47.21

torque ripple (Guohai et al., 2018). Given that the torque amplitude was large and unstable at start up, the waveform when the torque tends to be stable at 40 ms was selected for comparison. After optimisation, the fluctuation was significantly smaller. Compared with the initial torque ripple, it was reduced by 5.8% after optimisation, which made the motor operation more stable. Figure 10 represents a comparison chart of motor efficiency before and after optimisation, and the motor had the highest efficiency at a rated power of 15 kW. Through finite element simulation analysis, the initial efficiency of the motor increased from 94.2% to 96.6%. After optimisation, the efficiency of the motor was also improved while the cogging torque was reduced.

CONCLUSION

For the surface-mounted PMSM, this paper proposed a cogging torque optimisation method based on a combination of the Taguchi method and the response surface method. The method used the BA

Figure 8. Cogging torque before and after optimisation

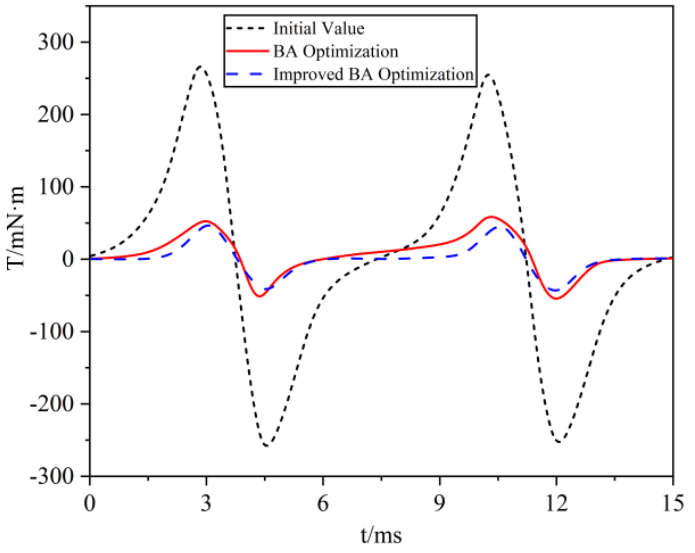

Figure 9. Torque ripple before and after optimisation

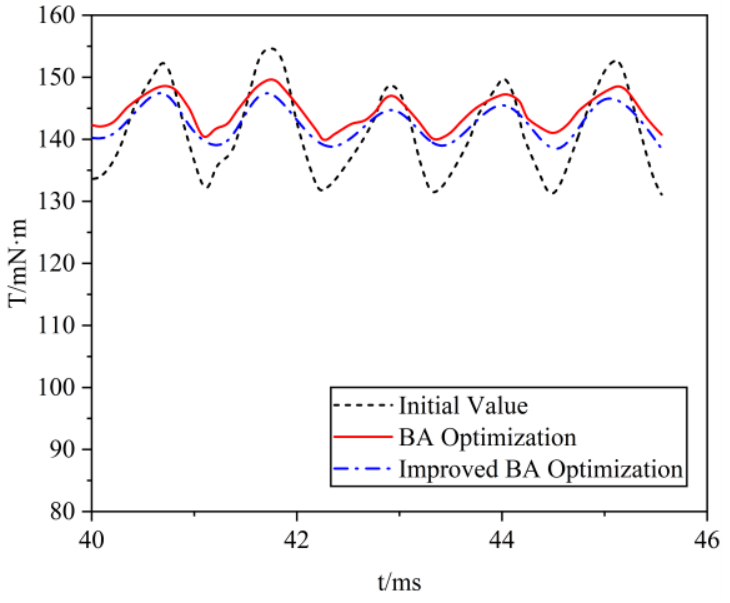

with Lévy flight feature to calculate optimal parameters and weaken the cogging torque. Furthermore, the finite element analysis method was applied to verify the motor performance before and after optimisation. The conclusions of this paper are summarised as follows:

1. The combination of the Taguchi method and the response surface method significantly improves the efficiency of optimising the motor cogging torque.

Figure 10. Motor efficiency before and after optimisation

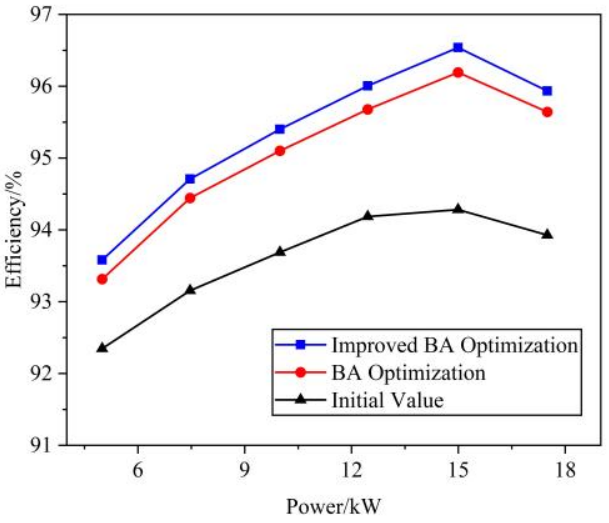

Compared with the single parameter optimisation methods, this combination can obtain optimised parameter values more accurately and quickly.

2. Optimisation of the motor structure parameters can significantly weaken the cogging torque and reduce torque ripple, thus reducing the motor noise.

The method proposed in this paper can effectively suppress the problem of excessive tooth slot torque in surface-mounted permanent magnet synchronous motors. However, the proposed method is only optimised for a single objective and cannot guarantee other optimal performances. Due to such limitations, further research is required on the multiobjective optimisation of motors.

AUTHOR NOTE

The data used to support the findings of this study are included within the article.

The authors declare that there is no conflict of interest regarding the publication of this paper.

This research received no external funding.

REFERENCES

Chen, S., Zhang, Z., & Li, J. X. (2021). Multi-objective optimization design of a permanent magnet synchronous motor based on Taguchi method. *Micromotors*, *54*(07), 17–22.

Cui, C. Y., Zhu, R. J., & Gong, X. J. (2021). Reactive power optimization of distribution network with distributed generation based on chaotic bat algorithm. *Electric Measurement and Instrument*, *58*(10), 95–100.

Deng, Q. L., & Liao, Y. Q., & Ai, W. H. (2022). Analysis and optimization of 8 kW disc-type permanent magnet motor cogging torque. *Journal of Hunan Institute of Engineering*, *32*(02), 13–18.

Feng, S., Qiu, H. B., & Huang, Y. C. (2023). *Optimization of cogging torque for miniature permanent magnet DC motors for vehicles*. Machinery Design & Manufacture.

Guo, L., Yao, S. C., & Ji, S. N. (2022). Application of Taguchi method in the optimal design of automotive permanent magnet synchronous motor. *Modern Electronic Technology*, *45*(5), 178–181.

Guohai, L., Yanyang, W., & Qian, C. (2018). Multi-objective optimization of an asymmetric V-shaped interior permanent magnet synchronous motor. *Transactions of China Electrotechnical Society*, *33*(S2), 385–393.

Hu, K., Wei, M., & Zhuang, H. J. (2020). Optimization design of interior permanent magnet synchronous motor based on compound algorithm. *Micromotor*, *53*(11), 50–55.

Jeihoon, B., Bonthu, S. S. R., & Seungdeog, C. (2016). Design of five-phase permanent magnet assisted synchronous reluctance motor for low output torque ripple applications. *IET Electric Power Applications*, *10*(5), 339–346. doi:10.1049/iet-epa.2015.0267

Jia, J. X., Yang, X. Y., & Cao, J. H. (2013). Optimization design of interior permanent magnet motor based on Taguchi method. *Micromotors*, *46*(6), 1–4.

Li, J. W., Zhang, X. Y., & Gao, T. (2022). Research on optimization method of cogging torque of U-type permanent magnet motor. *Journal of Chongqing University of Technology*, *36*(02), 107–114.

Li, M. M., Wang, Q. P., & Hui, H. (2021). Enhanced bat algorithm based on fractional-order strategy and spiral with Lévy flight. *Computer Engineering and Application*, *57*(18), 75–81.

Li, X. F., Gao, F. Y., & Qi, X. D. (2021). Cogging torque optimization of symmetrical V-type line-start permanent magnet synchronous motor. *Proceedings of the CSU-EPSA*, *33*(5), 1–8.

Luo, J., & Chen, X. H. (2021). Optimization of parameters for reducing cogging torque of marine permanent magnet motor based on multi-objective genetic algorithm. *Science & Technology Vision*, *351*(21), 136–138.

Ma, K., Jiang, X. F., & Liu, H. B. (2023). Torque optimization of permanent magnet fault-tolerant steering motor gears for electric vehicles based on rotor segmented diagonal poles. *Bulletin of Science and Technology*, *39*(02), 49–56.

Ma, K. R., Zhou, T., & Ji, J. (2022). Optimization analysis of cogging torque of permanent magnet synchronous motor. *Explosion-Proof Electric Machine*, *57*(02), 8–11.

Qiu, R. L. (2020). *Research on electromagnetic design and optimization of permanent magnet synchronous motor*. Qingdao University.

Qiu, R. L., Hua, Q. S., & Zhang, H. X. (2020). Optimal design of permanent magnet synchronous motor rotor based on Taguchi method. *Journal of Qingdao University (Engineering & Technology Edition), 35*(2), 57–61+82.

Song, W., Wang, X. H., & Yang, Y. B. (2004). New method for reducing cogging torque in surface-mounted permanent magnet motors. *Electric Machines and Control*, *8*(3), 214–217.

Tang, R. Y. (1997). *Theory and design of modern permanent magnet motor*. China Machine Press.

Wang, C. Z., Zhang, X. Y., & Wang, P. (2021). Optimization of cogging torque of double-layer embedded permanent magnet synchronous motor. *China Science Paper*, *16*(8), 906–910.

Wang, X. H., Li, Q. F., & Shi, S. (2002). Method of reducing cogging torque in permanent magnet motor. *Journal of Xi'an Jiaotong University*, *36*(06), 576–579.

Wang, X. H., Yang, Y. B., & Ding, T. T. (2005). The method for reducing cogging torque by suitable selection of pole-arc coefficient in solid-rotor PM synchronous motors. *Proceedings of the CSEE, 25*(15).

Wang, X. Y., Zhang, L., & Xv, W. G. (2016). Multi-objective optimal design for interior permanent magnet synchronous motor based on Taguchi method. *Micromotors*, *49*(05), 1–5.

Xiong, Z., & Fu, X. F. (2017). Isomeric bat algorithm for clustering. *Computer Engineering and Design, 38*(3), 677–681+728.

Xv, L. J., Mou, L., & Tang, L. (2020). Optimization of cogging torque of yokeless block split armature axial field permanent magnet motor based on response surface model and genetic algorithm. *Micromotors*, *53*(12), 22–28.

Yang, Y., Sun, Y., & Wang, X. D. (2022). Optimization of cogging torque of built-in V-type permanent magnet motor. *Modular Machine Tool and Automatic Machining Technology*, (12), 23–26.

Yang, Y. B., Wang, X. H., & Ding, T. T. (2007). Analysis of the optimization of the pole arc combination to reduce the cogging torque in PM motors. *Zhongguo Dianji Gongcheng Xuebao*, *27*(6), 7–11.

Yang, Y. S. Y., & Wang, X. D. (2023). Study on the cogging torque of built-in V-type permanent magnet motor with rotor structure optimization. *Modular Machine Tool and Automatic Machining Technology, 589*(3), 140–142+146.

Yao, X. J. (2023). Optimal design of the cogging torque of a permanent magnet DC motor for vehicles. *Agricultural Equipment & Vehicle Engineering*, *61*(3), 101–106.

Yao, Z. A., Chen, Y., & Liu, J. (2012). Study of PMSM tooth slot torque based on Taguchi method and rotor eccentricity. *Research and Exploration in Laboratory*, *41*(8), 102–106.

Zhang, L., Guo, H., & Yao, L. X. (2021). Research on microgrid optimization based on improved bat algorithm. *Power Grid and Clean Energy*, *37*(4), 122–126.

Zhang, Y. F., Zhang, X. Y., & Meng, X. Y. (2020). Optimization of magnetic pole parameters based on permanent magnet motor cogging torque. *Agricultural Equipment & Vehicle Engineering*, *58*(8), 9–11.

Zheng, Z. P., Jiang, W. L., & Hou, H. W. (2022). Optimization of cogging torque of permanent magnet drum based on finite element method. *Coal Technology*, *41*(4), 154–157.

Zhou, A. M. (2021). Optimal design of cogging torque of automatic door brushless DC motor. *Mechanical & Electrical Engineering Technology, 50*(4), 211–214+226.

Zhou, X. Y., Wang, D. P., & Xv, Z. K. (2020). Optimization of cogging torque of permanent magnet motor based on analytic-genetic algorithm. *Small and Special Electrical Machines*, *48*(11), 18–21.

Zou, J. J., Zhao, S. W., & Yang, X. Y. (2020). Genetic algorithm-based torque optimization of the outer rotor PMSM tooth slot. *Small and Special Electrical Machines*, *48*(4), 1–6.